Research on Chemical Intermediates
https://doi.org/10.1007/s11164-024-05285-7

Phosphorus–nitrogen compounds: part 75—design, synthesis, stereogenic and conformational properties of chiral dispiro(N/N)cyclotriphosphazenes: structural analysis and photophysical and bioactivity studies

Reşit Cemaloğlu[1,2] · Nuran Asmafiliz[1] · Zeynel Kılıç[1] · Burcu Topaloğlu Aksoy[3] · Büşra Nur Sabah[4] · Leyla Açık[4] · Tuncer Hökelek[5]

Received: 9 February 2024 / Accepted: 13 April 2024

Abstract

Multiheterocyclic inorganic–organic hybrid phosphazenes have robust inorganic ring systems with the stabilities of the phosphorus nitrogen skeleton and many different substituents bonded to the P atoms. In present study, unsymmetrical dispirocyclotriphosphazenes were prepared due to their potential to depict steric hindrance and electronic rearrangement in creating permanent chirality for certain conformational and configurational isomers. These isomers may have an effect on DNA bindings and activitiy against selected fungi and bacteria, remarkably. Herein, tetrachlorocyclotriphosphazenes (**1** and **2**) were reacted with 9-ethyl-N-methyl-3-carbazolyl-1,2-diaminoethane (**3**), 9-ethyl-N-ethyl-3-carbazolyl-1,2-diaminoethane (**4**) and 9-ethyl-N-methyl-3-carbazolyl-1,3-diaminopropane (**5**) to give the new unsymmetrical cis/trans-dispirocyclotriphosphazenes, [(ClBz/BzSpiro-6)R^1(N_3P_3)(CzSpiro-n)R^2]Cl_2 (Cz: Carbazolyl; R^1:Me R^2:Me or Et; n = 5 or 6; trans **6a**–**11a** and cis **6b**–**11b**). Characterizations, chiralities, and photophysical and biological properties of the new compounds were examined. The molecular and crystal structures of cis-**6b**, cis-**7b**, trans-**9a**, cis-**9b**, trans-**10a** and cis-**10b** were determined by single crystal X-ray crystallography. The chiralities of these compounds with unsymmetrical spiro-architectures were confirmed by X-ray crystallography. These results were further proven by ^{31}P NMR data recorded with the addition of a chiral solvent (CSA). Additionally, circular dichroism (CD) spectra also supported the results. Photophysical measurements indicate that these compounds show emission with lifetimes of approximately 5.6–5.9 ns. In addition, the bioactivities of some isomers were found to be different and quite high against some bacterial and yeast strains. Trans-**8a** was very active against *B. cereus* (MBC = 78.1 µM), while cis-**6b**, trans-**9a** and cis-**9b** were very active against the pathogenic yeast *C. albicans* (MFC = 156.3 µM).

Extended author information available on the last page of the article

Published online: 03 May 2024

Graphical abstract

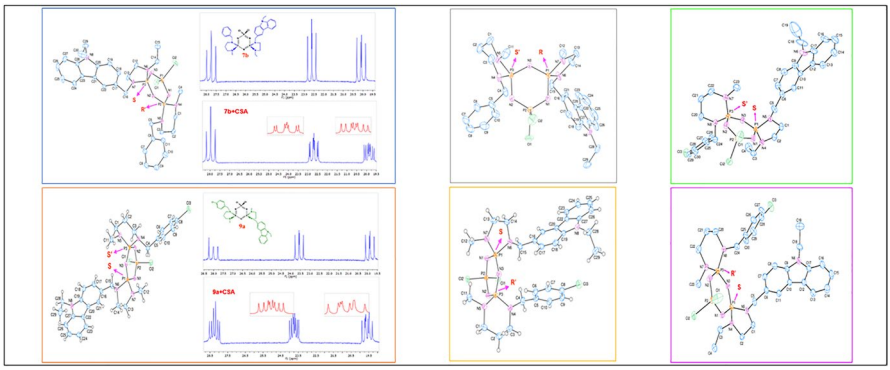

Keywords Unsymmetrical dispirocyclotriphosphazene · Crystal structure · Chirality · Photophysical properties · Antimicrobial activity

Introduction

Hexachlorocyclotriphosphazene (**HCCP**), trimer $(N{=}PCl_2)_3$, is one of the most significant, widely studied and renowned inorganic heterocyclic starting compound containing P=N units and active Cl atoms in its structure. Owing to the easy functionalization and reactivity of this compound, several reactions have been carried out, especially substitution reactions with nucleophiles such as aliphatic/aromatic diamines and dialkoxides/diphenoxides, yielding dispiro, trispiro, ansa, spiro-ansa, bino, spiro-bino and dangling architectures [1–11]. By appropriate nucleophilic substitution reactions, some phosphorus atoms to which nucleophiles bind can be converted into stereogenic centers. It is possible to examine the chiral properties of phosphazenes by single crystal X-ray crystallography, as well as using ^{31}P NMR spectra recorded with the addition of an optically active chiral solvating agent; (R)-(+)-2,2,2-trifluoro-1-(9'-antryl)-ethanol, CSA. The chiralities of these compounds are also confirmed by circular dichroism (CD) spectra in solution and chiral high-performance liquid chromatography (HPLC) [12–16].

However, phosphazene derivatives obtained from such reactions have a broad range of applications and uses, including chemical and biological recognition, sensing, imaging, flame retardancy, catalysis and biocompatible materials. Additionally, cyclotriphosphazenes and polyorganophosphazenes also serve as effective platforms in bioactivity studies such as antimicrobial agents in drug delivery, immunoadjuvants in tissue engineering, advanced anticancer therapies, and treatments for cardiovascular diseases [17].

On the other hand, enantiomerism (chirality) is a very important concept in drug design and development [18, 19]. Enantiomers are dissymmetric chiral molecules formed by bonding four different atoms and/or substituents to a central atom, and

whose mirror images cannot be fully superimposed and exhibit steric constraints [20, 21]. These restrictions can lead to very large reductions in rotation rates for bulky groups bonded to particular chiral centers [21]. The chirality of a drug's active molecule significantly affects its pharmacodynamics, pharmacokinetics and toxicity properties [22]. Some of the drugs are sold as chiral pure enantiomers, usually exhibiting the most active chiral isomer, while others are sold as racemic mixtures. Drugs such as perhexiline, thalidomide and ibuprofen are the most classical examples [23–29].

Therefore, this study aims to synthesize new and effective bioactive chiral compounds due to the structural and unique biological properties of phosphazene derivatives. Carbazole and substituted carbazole scaffolds are nitrogen-containing planar heterocyclic pharmacophores in therapeutic chemistry. They also have remarkable biological properties such as antibacterial, antitumor, anti-inflammatory, antioxidant and antifungal activities [30–34]. Carbazole derivatives have an important place not only in bioactivity research but also in photophysical studies [35, 36]. To the best of our knowledge, based on the literature survey, there is only one report on monospirocyclotriphosphazenes decorated with carbazolyldiamines [37] and only two reports of unsymmetrical dispirocyclotriphosphazenes decorated with carbazolyldiamines [14, 38]. Therefore, in this study, carbazole and biocompatible phosphazenes were combined to obtain new effective cyclotriphosphazenes and to examine their bioactivities. The new unsymmetrical cis/trans-dispiro(N/N)cyclotriphosphazenes, trans-(**6a**–**11a**) and cis-(**6b**–**11b**), with different bulky side groups were obtained and their spectroscopic, crystallographic, photophysical and chiral properties were determined.

Experimental

The details of materials and methods and X-ray crystallography were moved to the Supplementary Information (SI).

Preparations of the compounds

Tetrachloromonospirocyclotriphosphazenes (**1** and **2**) and diamines (**3**–**5**) were obtained according to the published papers [6, 37, 39].

Syntheses of 6a and 6b

Tetrachloromonospirophosphazene (**1**) in THF (2.85 g, 6.30 mmol) was added to the solution of carbazolyldiamine (**3**) (1.77 g, 6.30 mmol) and triethylamine (Et_3N; 1.75 mL, 12.60 mmol) in tetrahydrofuran (THF) at room temperature. The reaction proceeded for 3 days at room temperature. During this period, the reaction medium was monitored by thin layer chromatography. The reaction is completed with product formation. Triethylammonium chloride salt was removed by filtration. THF was then evaporated and pure dispirophosphazenes were isolated by column

chromatography (toluene-THF: 5/1). Firstly, the trans-**6a** was obtained. Yield: 1.32 g, 2.00 mmol (32%), m.p.: 124 °C, Rf: 0.38 (toluene-THF: 5/1). Then, the cis-**6b** compound was isolated. Yield: 1.18 g, 1.78 mmol (28%), m.p.: 141 °C, Rf: 0.27 (toluene-THF: 5/1). Elemental Analysis (**6a**): Anal. calc. for $P_3N_8Cl_2C_{29}H_{37}$ (%): C: 52.66, H: 5.64, N: 16.94; Found (%): C: 52.45, H: 5.81, N: 16.79. FTIR (**6a**): ν 3028 (C–H arom.), 2922 (asym.), 2845 (sym.) (C–H aliph.), 1131 (asym.) (P=N), 572 (asym.), 534 (sym.) (P–Cl aliph.). APIES-MS (fragments are based on ^{35}Cl, Ir %): m/z calc. 661.59 ($[MH]^+$, 100.0). Found: 661.65 ($[MH]^+$, 100.0). Elemental Analysis (**6b**): Anal. calc. for $P_3N_8Cl_2C_{29}H_{37}$ (%): C: 52.66, H: 5.64, N: 16.94; Found (%): C: 52.37, H: 5.81, N: 16.52. FTIR (**6b**): ν 3054 (C–H arom.), 2937 (asym.), 2846 (sym.) (C–H aliph.), 1162 (asym.) (P=N), 569 (asym.), 539 (sym.) (P–Cl aliph.). APIES-MS (fragments are based on ^{35}Cl, Ir %): m/z calc. 661.59 ([MH]+, 100.0). Found: 661.67 ([MH]+, 100.0).

Syntheses of 7a and 7b

In order to synthesize **7a** and **7b**, the same procedure performed in the syntheses of **6a** and **6b** was implemented. Monospirophosphazene compound (**1**) (3.00 g, 6.64 mmol) in THF was added into the solution containing carbazolyldiamine compound (**4**) (1.96 g, 6.64 mmol) and triethylamine (Et_3N; 1.85 mL, 13.28 mmmol). Firstly, the trans-**7a** compound was obtained by column chromatography. Yield: 2.10 g, 3.12 mmol (47%), m.p.: 107 °C, Rf: 0.31 (toluene-THF: 5/1). Then, the cis-**7b** compound was isolated in pure form. Yield: 1.64 g, 2.44 mmol (37%), m.p.: 118 °C, Rf: 0.24 (toluene-THF: 5/1). Elemental Analysis (**7a**): Anal. calc. for $P_3N_8Cl_2C_{30}H_{39}$ (%): C: 53.34, H: 5.82, N: 16.59; Found (%): C: 53.05, H: 5.71, N: 16.38. FTIR (**7a**): ν 3057 (C–H arom.), 2966 (asym.), 2842 (sym.) (C–H aliph.), 1123 (asym.) (P=N), 573 (asym.), 531 (sym.) (P–Cl aliph.). QTOF-MS (fragments are based on ^{35}Cl, Ir %): m/z calc. 675.20 ($[MH]^+$, 100.0). Found: 675.19 ($[MH]^+$, 100.0). Elemental Analysis (**7b**): Anal. calc. for $P_3N_8Cl_2C_{30}H_{39}$ (%): C: 53.34, H: 5.82, N: 16.59; Found (%): C: 53.01, H: 5.88, N: 15.93. FTIR (**7b**): ν 3057 (C–H arom.), 2969 (asym.), 2844 (sym.) (C–H aliph.), 1123 (asym.) (P=N), 567 (asym.), 538 (sym.) (P–Cl aliph.). QTOF-MS (fragments are based on ^{35}Cl, Ir %): m/z calc. 675.20 ($[MH]^+$, 100.0). Found: 675.19 ($[MH]^+$, 100.0).

Syntheses of 8a and 8b

The exact same procedure performed in the syntheses of **6a** and **6b** was implemented to synthesize compounds **8a** and **8b**. Triethylamine (Et_3N; 1.85 mL, 13.28 mmol) was added into the solution prepared by dissolving the carbazolyldiamine (**5**) (1.96 g, 6.64 mmol) in THF. Then, the solution of monospirophosphazene (**1**) (3.00 g, 6.64 mmol) in THF was added into this solution. Firstly, the trans-**8a** compound was obtained using column chromatography. Yield: 2.08 g, 3.08 mmol (46%), m.p.: 126 °C, Rf: 0.42 (toluene-THF: 5/1). Then, the cis-**8b** compound was obtained in pure form. Yield: 1.58 g, 2.34 mmol (35%), m.p.: 111 °C, Rf: 0.32 (toluene-THF: 5/1). Elemental Analysis (**8a**): Anal. calc. for $P_3N_8Cl_2C_{30}H_{39}.1/2C_4H_8O$ (%): C:

54.01, H: 6.09, N: 15.75; Found (%): C: 53.80, H: 6.13, N: 16.07. FTIR (**8a**): ν 3031 (C–H arom.), 2973 (asym.), 2845 (sym.) (C–H aliph.), 1115 (asym.) (P=N), 562 (asym.), 537 (sym.) (P–Cl aliph.). QTOF-MS (fragments are based on ^{35}Cl, Ir %): m/z calc. 675.20 ($[MH]^+$, 100.0). Found: 675.21 ($[MH]^+$, 100.0). Elemental Analysis (**8b**): Anal. calc. for $P_3N_8Cl_2C_{30}H_{39}$ (%): C: 53.34, H: 5.82, N: 16.59; Found (%): C: 53.74, H: 5.90, N: 16.18. FTIR (**8b**): ν 3031 (C–H arom.), 2974 (asym.), 2845 (sym.) (C–H aliph.), 1115 (asym.) (P=N), 562 (asym.), 535 (sym.) (P–Cl aliph.). QTOF-MS (fragments are based on ^{35}Cl, Ir %): m/z calc. 675.20 ($[MH]^+$, 100.0). Found: 675.20 ($[MH]^+$, 100.0).

Syntheses of 9a and 9b

The same procedure performed in the syntheses of **6a** and **6b** was carried out to synthesize compounds **9a** and **9b**. The solution of the compound tetrachloromonospirophosphazene (**2**) (3.20 g, 6.58 mmol) in THF, was added into the solution containing carbazolyldiamine compound (**3**) (1.85 g, 6.58 mmol) and triethylamine (Et_3N; 1.83 mL, 13.16 mmol). Firstly, the trans-**9a** compound was obtained by column chromatography. Yield: 2.36 g, 3.40 mmol (52%), m.p.: 132 °C, Rf: 0.29 (toluene-THF: 5/1). Then, the cis-**9b** compound was isolated in pure form. Yield: 1.58 g, 2.28 mmol (35%), m.p.: 102 °C, Rf: 0.21 (toluene-THF: 5/1). Elemental Analysis (**9a**): Anal. calc. for $P_3N_8Cl_3C_{29}H_{36}.1/2H_2O$ (%): C: 49.41, H: 5.29, N: 15.90; Found (%): C: 49.40, H: 5.24, N: 15.48. FTIR (**9a**): ν 3054 (C–H arom.), 2973 (asym.), 2850 (sym.) (C–H aliph.), 1123 (asym.) (P=N), 563 (asym.), 529 (sym.) (P–Cl aliph.). HR-MS (fragments are based on ^{35}Cl, Ir %): m/z calc. 695.59 ($[MH]^+$, 100.0). Found: 695.15 ($[MH]^+$, 100.0). Elemental Analysis (**9b**): Anal. calc. for $P_3N_8Cl_3C_{29}H_{36}$ (%): C: 50.05, H: 5.21, N: 16.10; Found (%): C: 50.63, H: 5.10, N: 16.10. FTIR (**9b**): ν 3053 (C–H arom.), 2969 (asym.), 2866 (sym.) (C–H aliph.), 1159 (asym.) (P=N), 567 (asym.), 535 (sym.) (P–Cl aliph.). HR-MS (fragments are based on ^{35}Cl, Ir %): m/z calc. 695.59 ($[M+H]^+$, 100.0). Found: 695.15 ($[M+H]^+$, 100.0).

Syntheses of 10a and 10b

The same procedure performed in the syntheses of **6a** and **6b** was carried out to synthesize compounds **10a** and **10b**. Monospirophosphazene (**2**) (2.88 g, 5.93 mmol) in THF was added into the solution containing carbazolyldiamine compound (**4**) (1.75 g 5.93 mmol) and triethylamine (Et_3N; 1.65 mL, 11.86 mmmol). Initially, the trans-**10a** compound was obtained by column chromatography method. Yield: 1.74 g, 2.46 mmol (41%), m.p.: 99 °C, Rf: 0.33 (toluene-THF: 5/1). Then, the cis-**10b** compound was isolated in pure form. Yield: 1.42 g, 2.00 mmol (34%), m.p.: 127 °C, Rf: 0.23 (toluene-THF: 5/1). Elemental Analysis (**10a**): Anal. calc. for $P_3N_8Cl_3C_{30}H_{38}$ (%): C: 50.75, H: 5.39, N: 15.78; Found (%): C: 50.92, H: 5.57, N: 15.56. FTIR (**10a**): ν 3052 (C–H arom.), 2971 (asym.), 2867 (sym.) (C–H aliph.), 1149 (asym.) (P=N), 571 (asym.), 536 (sym.) (P–Cl aliph.). QTOF-MS (fragments are based on ^{35}Cl, Ir %): m/z calc. 709.16 ($[MH]^+$, 100.0). Found: 709.15 ($[MH]^+$,

100.0). Elemental Analysis (**10b**): Anal. calc. for $P_3N_8Cl_3C_{30}H_{38}$ (%): C: 50.75, H: 5.39, N: 15.78; Found (%): C: 50.46, H: 5.54, N: 15.65. FTIR (**10b**): ν 3051 (C–H arom.), 2973 (asym.), 2856 (sym.) (C–H aliph.), 1156 (asym.) (P=N), 570 (asym.), 535 (sym.) (P–Cl aliph.). QTOF-MS (fragments are based on ^{35}Cl, Ir %): m/z calc. 709.16 ($[MH]^+$, 100.0). Found: 709.16 ($[MH]^+$, 100.0).

Syntheses of 11a and 11b

The same procedure performed in the syntheses of **6a** and **6b** was applied to synthesize compounds **11a** and **11b**. Triethylamine (Et_3N; 1.76 mL, 12.68 mmol) was added into the solution prepared by dissolving the carbazolyldiamine (**5**) (1.87 g, 6.34 mmol) in THF. Then, the monospirophosphazene (**2**) solution prepared by dissolving (3.08 g, 6.34 mmol) in THF was added into this solution. Firstly, the trans-**11a** compound was obtained applying column chromatography. Yield: 2.46 g, 3.48 mmol (55%), m.p.: 135 °C, Rf: 0.39 (toluene-THF: 5/1). Then, the cis-**11b** compound was isolated in pure form. Yield: 1.52 g, 2.14 mmol (34%), m.p.: 147 °C, Rf: 0.31 (toluene-THF: 5/1). Elemental Analysis (**11a**): Anal. calc. for $P_3N_8Cl_3C_{30}H_{38}$ (%): C: 50.75, H: 5.39, N: 15.78; Found (%): C: 50.56, H: 5.67, N: 15.52. FTIR (**11a**): ν 3051 (C–H asym.), 2940 (asim.), 2838 (sym.) (C–H aliph.), 1130 (asym.) (P=N), 589 (asym.), 535 (sym.) (P–Cl aliph.). APIES-MS (fragments are based on ^{35}Cl, Ir %): m/z calc. 709.61 ($[MH]^+$, 100.0). Found: 709.72 ($[MH]^+$, 100.0). Elemental Analysis (**11b**): Anal. calc. for $P_3N_8Cl_3C_{30}H_{38}$ (%): C: 50.75, H: 5.39, N: 15.78; Found (%): C: 50.90, H: 5.69, N: 15.42. FTIR (**11b**): ν 3051 (C–H arom.), 2936 (asym.), 2845 (sym.) (C–H aliph.), 1122 (asym.) (P=N), 575 (asym.), 533 (sym.) (P–Cl aliph.). APIES-MS (fragments are based on ^{35}Cl, Ir %): m/z calc. 709.61 ($[MH]^+$, 100.0). Found: 709.63 ($[MH]^+$, 100.0).

Additionally, methods for determination of antimicrobial and antioxidant activities, MIC and MBC/MFC values, cytotoxicity assay, DNA-compound interactions and *BamH*I and *Hind*III digestion were presented in Supplementary Information (SI). The ^{1}H, ^{13}C, ^{31}P NMR and mass spectra of all the dispirophosphazenes were also given in the SI.

Results and discussion

Syntheses of unsymmetrical dispirocyclotriphosphazenes

Syntheses of unsymmetrical dispirocyclotriphosphazenes were carried out by the following steps. According to the published procedure, the starting compounds, monospirocyclotriphosphazenes (**1** and **2**), were obtained from the reactions of **HCCP** and (benzyl/chlorobenzyl)diamines [6, 39]. Meanwhile, for use as ligands, carbazolyldiamines (**3**, **4** and **5**) produced from the condensation reactions of 9-ethyl-3-carbazolecarboxaldehyde with N-methyl-1,2-diaminoethane, N-ethyl-1,2-diaminoethane and N-methyl-1,3-diaminopropane [37]. In THF, the regioselective nucleophilic substitution reactions of monospirocyclotri-phosphazenes

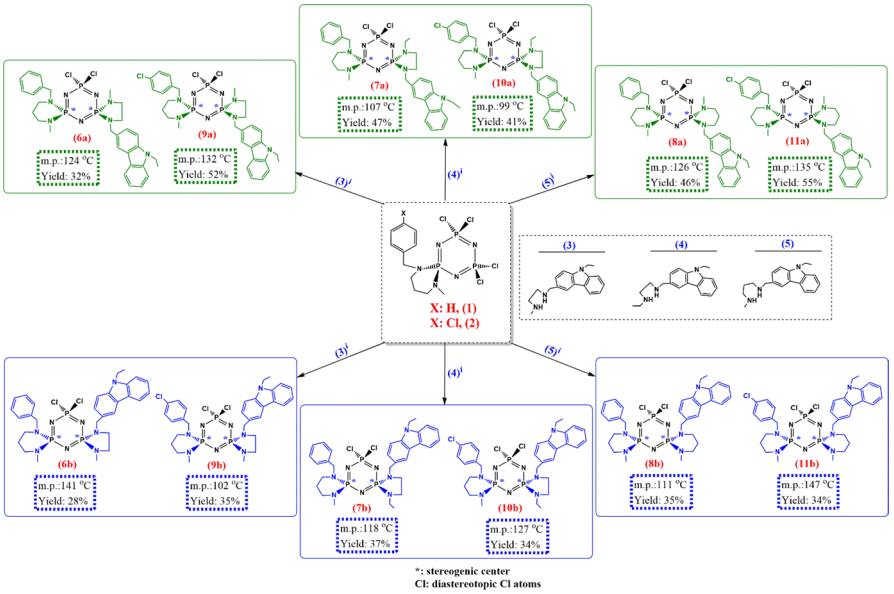

Scheme 1: The condensation reactions of tetrachloro(benzyl/4-chlorobenzyl) (N/N)spirocyclotriphosphazenes with the carbazolyldiamines. (i) Reactions were made using Et_3N in THF at room temperature

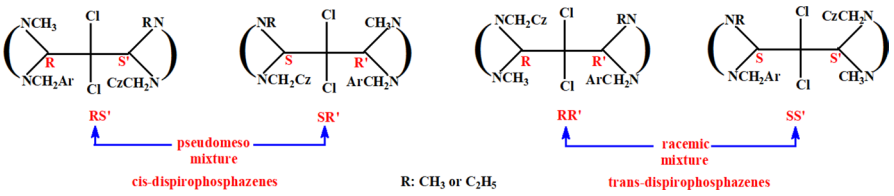

Fig. 1 The expected chiral isomer distributions of the cis and trans dispirophosphazenes

(**1** and **2**) and diamines (**3**, **4** and **5**) in equimolar amounts yielded respectively, unsymmetrical cis (**6a**–**11a**) and trans (**6b**–**11b**) dispirocyclotriphosphazenes containing carbazolyl and benzyl/4-chloro-benzyl pendant arms (Scheme 1). Cis/trans-isomers occur due to the spatial positions of NMe or NEt groups bonded to the spiro rings. All the cis and trans geometrical isomers were purified using silica gel as an adsorbent in column chromatography. According to R_f values, the retention times of cis-isomers are slightly longer than those of the trans-isomers. The yields of trans-dispirophosphazenes were found to be higher than those of cis-dispirophosphazenes. This may be due to the fact that the steric hindarances of the bulky side groups of cis-isomers are greater than those of trans-isomers. More importantly, in trans and cis-dispiro-cyclotriphosphazenes, centers containing chiral P-atoms with R and/or S configurations emerge (Fig. 1).

According to Fig. 1, as a mixture of enantiomers, RS' and SR' is not a classical **mesosystem** due to the lack of a plane of symmetry. However, considering the presence of RS' and SR' enantiomers, such a mixture can be described as a "**pseudomeso system**" [40, 41].

There are a few reports in the literature about non-symmetrical dispirocyclotriphosphazenes without pendant arms [42–46]. Moreover, to our knowledge, only three articles have been found on dispirocyclo-triphosphazenes containing different unsymmetrical pendant arms [14, 38, 47]. The scarcity of studies on unsymmetrically substituted dispirocyclotriphosphazenes raises the significance of this current study. The spectroscopic properties of these novel dispirophosphazenes were elucidated using ^{31}P, ^{1}H and ^{13}C NMR, FTIR and MS spectral data. The results are consistent with the proposed dispirocyclotriphosphazene formulae. In addition, due to the different pendant-armed spiro groups bonded to P-atoms, unsymmetrical cis-dispirocyclotriphosphazenes (**6b–11b**) are expected to exist as "pseudomeso racemate" (RS'/SR') and trans-dispirocyclotriphosphazenes (**6a–11a**) as "racemate" (RR'/SS') [48]. As examples, the chiral properties of dispirophosphazenes (**cis-7b** and **trans-9a**) were examined by CSA-added ^{31}P NMR spectroscopy. When the molar ratio of phosphazene to CSA was 1:10, the effects of CSA on the ^{31}P NMR spectra of the two dispirophosphazenes were visualized in Fig. 2. As expected, different NMR signals appeared for the enantiomers due to the formation of diastereomeric adducts in solution as a result of the solvation reaction between the chiral dispirophosphazene and the chiral ligand, CSA. It was observed that after the addition of CSA, the peaks of the racemates were split into two lines belonging to two different enantiomers. These outputs are the evidences of the dispirophosphazenes exist in racemates. In addition, enantiomeric separations were clearly defined and the calculated results were listed in Table 1.

Additionally, when the CD spectra were examined to evaluate the chiral properties of non-symmetrical dispirophosphazenes, positive and negative cotton effects were observed in all spectra. The observation of both positive and negative cotton

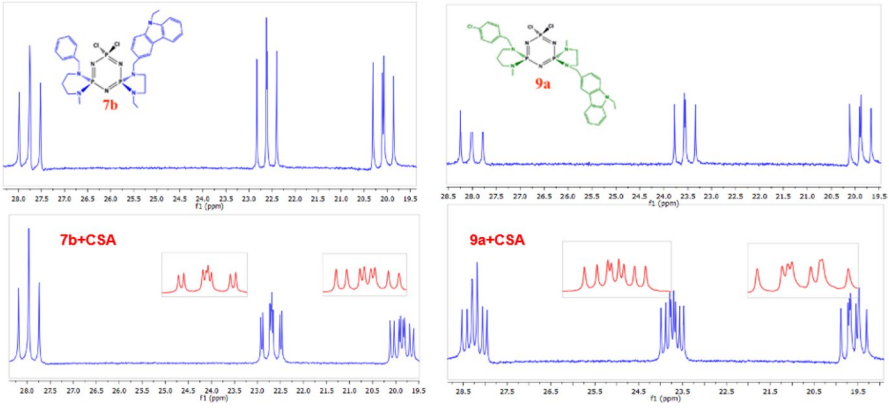

Fig. 2 The ^{1}H decoupled ^{31}P NMR spectra of phosphazenes (cis-**7b** and trans-**9a**) and the addition of CSA at ca. 10:1 mol ratio showing the enantiomers

Table 1 The ^{31}P NMR (decoupled) spectral data of two phosphazenes and the effects of CSA on ^{31}P NMR chemical shifts

Chemical shifts/ppm				
Compound	PCl_2	P(NN/benzyl)	P(NN/carbazolyl)	$^2J_{PP}$/Hz
(i) ^{31}P NMR spectral data				
cis-7b	27.76	22.62	20.09	48.6
				48.6
				46.2
trans-9a	28.01	23.56	19.90	48.6
				46.2
				43.7
(ii) Effect of CSA on ^{31}P NMR chemical shifts (ppb) at a 10:1 mol ratio				
cis-7b	+209	+99	−190	49.7
				42.8
				41.8
trans-9a	+283	+213	−227	47.5
				43.7
				41.4
(iii) Separation of enantiomeric signals (ppb) at a 10:1 mol ratio of CSA:molecule				
cis-7b	–	42	86	
trans-9a	112	100	165	

202.46 MHz ^{31}P NMR measurements in $CDCl_3$ solutions at 293 K

effects in the spectra (Fig. S1) proves that cis and trans dispirophosphazenes exist as racemates in solution, as reported in the literature, previously [10, 25]. As examples, the CD spectra of **cis-7b** and **trans-9a** are given in Fig. S2.

Also, the absolute configurations of one enantiomer of each of the cis-**6b**, cis-**7b**, trans-**9a**, cis-**9b**, trans-**10a** and cis-**10b** isomers were found to be as RS', RS', SS', SR', SS' and SR', respectively, by X-ray data. Therefore, it can be concluded that the results of evaluating the chirality obtained by CSA added-^{31}P NMR spectroscopy, X-ray crystallography and CD techniques are in harmony with each other. On the other hand, FTIR, APIES-MS, microanalytical and NMR analysis results also support the proposed structures. Protonated molecular ion peaks $[MH]^+$ are present in the MS spectra of all phosphazenes.

NMR and IR spectroscopies

^{31}P, ^{13}C and ^{1}H NMR techniques are widely used to determine the spectroscopic properties of dispirophosphazene derivatives. Among these, ^{31}P NMR spectroscopy provides the most essential data about the structures of phosphazenes. In particular, ^{13}C and ^{1}H NMR spectra are also very useful to prove that nucleophilic substitution reactions occur. Herein, the proton-decoupled ^{31}P NMR spectra of dispirophosphazenes (**6a–11b**) were evaluated in detail. $^{31}P(^{1}H)$ NMR data were listed in

Table S1. Dichlorodispirophosphazenes chemically have three different phosphorus atoms. The chemical shifts of the P(spiro/carbazolyl) and P(spiro/benzyl) nuclei of the compounds differ slightly from each other due to their similar chemical environments. The peaks of all phosphorus atoms except trans-(**8a/11a**) and cis-(**8b/11b)** emerge as doublets of doublets. The unexpected resonance of P(NN/Bz) and P(NN/Cz) phosphorus atoms in the structures of **8a/8b** and **11a/11b** at the same chemical shifts indicates that their spin systems are AX_2. Therefore, for these six-membered dispirophosphazenes, triplets and doublets signals appear. The spin systems of other phosphazenes with five-membered P(spiro/carbazolyl) and six-membered P(spiro/benzyl) dispiro-rings were determined as AMX. In addition, the P(NN/Bz) and PCl_2 phosphorus atoms of dispirophosphazenes (**8a/8b** and **11a/11b**) resonate at a higher magnetic field (lower chemical shift) compared to other ones.

On the other hand, the spin–spin coupling constants of dispirophosphazenes, $^{2}\boldsymbol{J}_{\mathbf{PP}}$, were calculated between 36.4 and 51.0 Hz. In general, the $^{2}\boldsymbol{J}_{\mathbf{PP}}$ values of cis-dispirophosphazenes are slightly smaller than those of trans-dispirophosphazenes. Additionally, the average $^{2}\boldsymbol{J}_{\mathbf{PP}}$ constants of dispirophosphazenes with 5-membered and 6-membered spiro-rings were calculated as 46.6 Hz and 37.4 Hz, respectively [14, 38].

On the other hand, the chemical shifts of the protons and carbons of dispirophosphazenes, coupling constants and multiplicities were scrutinized together (Tables S2 and S3). Characteristic signals providing important information about nucleophilic substitution reactions were detected from ^{13}C NMR spectra. The signals appearing in the ranges of 50.38–50.95 ppm and 49.78–50.74 ppm are attributed to carbazolyl (Cz**C**H_2) and benzyl (Ph**C**H_2) carbons. Likewise, signals belonging to the ipso-carbons of benzyl (C1) and carbazolyl rings (C1') in the structures are present in the ranges of 136.44–138.38 ppm and 127.15–128.39 ppm, respectively. These peaks occur as doublets due to phosphorus–carbon spin–spin couplings. The average coupling constants of $^{2}\boldsymbol{J}_{\mathrm{PC}}$ (for Cz**C**H_2) and $^{2}\boldsymbol{J}_{\mathrm{PC}}$ (for Ph**C**H_2), and $^{3}J_{\mathrm{PC1}}$ and $^{3}\boldsymbol{J}_{\mathrm{PC1'}}$ of the dispirophosphazenes were found to be 7.9 Hz and 7.7 Hz, respectively.

The N**C**H_2, NCH_2**C**H_2, CH_3N**C**H_2 carbons in the spiro rings resonate at the expected chemical shifts. In addition, the average $^{2}\boldsymbol{J}_{\mathrm{PC}}$ value of the five-membered spiro products was calculated as 12.6 Hz and it is consistent with the reported literature values [14, 38]. It has been also determined that the N**C**H_2 (C_d) carbons present in the structure of the (benzyl/chlorobenzyl)diamine ligands resonate in the range of 48.97–50.44 ppm (Table S2). These signals are observed as doublets for compounds **6a/6b**, **7a/7b**, **9a/9b**, **10a/10b** (average $^{3}\boldsymbol{J}_{\mathrm{PC}} = 4.7$ Hz). Moreover, the peaks of the N**C**H_3 carbons (C_a and C_e) found in the diamine ligands of all compounds appear in the range of 31.63–36.12 ppm. The signals belonging to the NCH_2**C**H_3 carbons in the carbazole ring emerge as singlets between 13.80 and 13.86 ppm. Characteristic signals of other aromatic and aliphatic carbon atoms in the structures were evaluated at the expected chemical shifts [14, 38].

On the other hand, all characteristic signals of aliphatic and aromatic protons are seen in the ^{1}H NMR spectra of dispirophosphazenes (Table S3). It was determined that benzylic protons (PhC**H**$_2$) resonate in the range of 4.07–4.38 ppm. In trans-compounds **6a, 7a, 8a, 9a, 10a**, **11a** and in **cis-9b** these signals appear in doublets as a result of phosphorus–proton spin–spin couplings (average $^{3}\boldsymbol{J}_{\mathrm{PH}} = 7.2$ Hz). For

cis-compounds (except **9b**) **6b**, **7b**, **8b**, **10b** and **11b**, PhC**H**$_2$ protons were determined to be diastereotopic protons (protons that are not equivalent with respect to the electronic environment). The signals of these diastereotopic protons appear as a doublet of doublets (dd) as a result of P and H spin–spin (average $^3J_{PH}$ = 7.5 Hz), and H and H spin–spin couplings (average $^2J_{HH}$ = 14.3 Hz). Carbazolyl protons (CzC**H**$_2$) existing in all compounds were determined as doublet of doublets as a result of vicinal and geminal couplings in the range of 3.91–4.24 ppm (average $^3J_{PH}$ = 7.8 Hz and $^2J_{HH}$ = 14.9 Hz). In all compounds, the signals of NC**H**$_3$ protons in benzyl and carbazolyldiamino precursors are found in doublets in the range of 2.63–2.72 ppm (average $^3J_{PH}$ = 11.6 Hz) and 2.50–2.68 ppm (average $^3J_{PH}$ = 13.3 Hz), respectively. The peaks of NC**H**$_2$CH$_3$ protons in the carbazole ring appear as quadruplets in the range of 4.33–4.39 ppm (average $^3J_{HH}$ = 7.2 Hz). In addition, the protons of the phenyl and carbazole rings resonate in the ranges of 7.02–7.40 ppm and 7.02–8.15 ppm, respectively. As a result, all these characteristic data found by ^{31}P, ^{13}C and ^{1}H NMR spectroscopy analyses prove that the trimeric phosphazene ring undergoes substitution reactions.

Characteristic FTIR frequencies of the dispirophosphazenes are presented in the "Experimental Section". Likewise, the detected absorption bands of compounds verify the substitution of **HCCP** with diamines. In general, strong ν(asymm.) and ν(symm.) vibrations of νPN of dispirocyclotriphosphazenes were observed in the ranges of approximately 1250–1200 cm^{-1} and 1115–1162 cm^{-1}. The bands observed for dichlorodispirophosphazenes between 529 and 589 cm^{-1} are attributed to P–Cl bonds, which favor partial substitution of **HCCP**. Additionally, aromatic C–H stretching vibrations were determined to be 3028–3057 cm^{-1}. All these findings are compatible with literature data [14, 38].

Photophysical properties

The optical properties of all cis/trans-dispirocyclotriphosphazenes were examined by both steady-state and time-resolved fluorescence spectroscopy techniques. Electronic absorption and emission behaviors of dispirophosphazenes (trans-**6a**, cis-**6b**, trans-**7a**, cis-**7b**, cis-**8b**, trans-**9a**, cis-**9b**, trans-**10a**, cis-**10b**, trans-**11a** and cis-**11b**) were evaluated in different polar and non-polar solvents such as dichloromethane, acetonitrile, acetone, toluene and ethyl acetate. Studies were carried out to determine the most suitable solvent in terms of solubility and photophysical properties. According to the results obtained, dichloromethane was selected as the most suitable solvent (Fig. S3). In the absorption spectra of the dispirophosphazenes, the absorptions corresponding to wavelengths of 265 nm, 295 nm, 335 nm and 350 nm were associated with the π–π* and n–π* transitions in the optically active carbazole skeleton of the compounds. All dispirophosphazenes display emission corresponding to wavelengths of 360 nm and 370 nm when excited at a wavelength of 290 nm (Fig. 3 and Fig. S4). When these results were evaluated, it was concluded that the absorption and emission behaviors of the compounds were due to the carbazole ring, since the cyclotriphosphazene ring was optically inert [49–52]. This result suggests that the carbazole rings do not have an effective ground-state interaction. In fact,

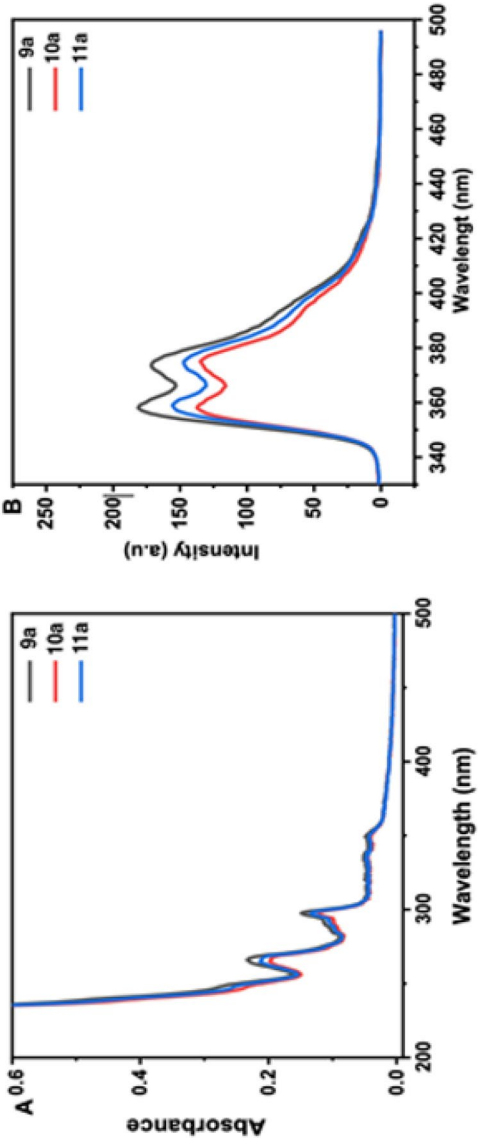

Fig. 3 Optical absorption and fluorescence emission spectra of trans-**9a**, **10a**, **11a** (**A**, **B**) isomers in DCM (5×10^{-6} M; ex: 290 nm)

fluorescence lifetime, τ_F (ns), is a critical parameter in fluorescence spectroscopy and is widely used to probe the local environment and interactions of a fluorophore. The fluorescence lifetimes of the dispirophosphazenes were determined by the time-correlated single photon counting (**TCSPC**) technique. All lifetime studies were performed in dichloromethane by excitation of the compounds at 310 nm (Table 2). The fluorescence decay profiles of the compounds (**6a/6b**, **7a/7b**, **8b**, **9a/9b**, **10a/10b** and **11a/11b**) in DCM with excitation at 310 nm are visualized in Fig. S5. According to the data obtained by this method, it is understood that the compounds have emission profiles varying between 5.6 and 5.9 ns (Fig. S5). The fluorescence half-life time, τ_F (ns), and chi-square test (CHISQ) values of cis-isomers (**6b–11b**) are also considerably larger than those of trans-isomers (**6a–11a**) (Table 2). This can be attributed to the fact that cis-isomers form more ordered aggregates in solution. Compared to the literature data, it can be concluded that these compounds have a very long fluorescence half-life [14, 38].

X-ray structures of 6b, 7b, 9a, 9b, 10a and 10b

The crystal structures of cis-**6b**, cis-**7b**, trans-**9a**, cis-**9b**, trans-**10a** and cis-**10b** isomers were enlightened by single crystal X-ray crystallography. The ORTEP diagrams of cis-**6b**, cis-**7b**, trans-**9a**, cis-**9b**, trans-**10a** and cis-**10b** isomers along with atom numbering schemes are visualized in Figs. 4, 5, 6, 7, 8 and 9. Experimental details are given in Table S4. Herein, dispirophosphazenes are described as cis- or trans-isomers according to the orientations of the N-R groups (R: Me and/or Et) in the different spiro rings. Conformations of the trimeric phosphazene rings, (P1/N1/P2/N2/P3/N3), rings were determined as flattened-boat for compounds (cis-**6b**, cis-**7b**, trans-**9a,** trans-**10a** and cis-**10b**) [Fig. S6a; $Q_T = 0.027(2)$ Å, $\varphi_2 = 70.8(2.6)°$ and $\theta_2 = 75.0(2.4)°$ (for **6b**), Fig. S7a; $Q_T = 0.052(2)$ Å, $\varphi_2 = 23.0(2.6)°$ and $\theta_2 = 114.4(2.2)°$ (for **7b**), Fig. S8a; $Q_T = 0.144(1)$ Å, $\varphi_2 = 52.7(4)°$ and $\theta_2 = 75.9(4)°$ (for **9a**) and Fig. S9a; $Q_T = 0.175(2)$ Å, $\varphi_2 = -49.8(8)°$ and $\theta_2 = 110.6(6)°$ (for **10a**) and Fig. S11a; $Q_T = 0.107(1)$ Å, $\varphi_2 = 45.3(7)°$ and $\theta_2 = 86.2(7)°$ (for **10b**)] and screw-boat for compound **9b** [Fig. S10a; $Q_T = 0.129(1)$ Å, $\varphi_2 = 85.3(5)°$, $\theta_2 = 67.8(5)°$ (for **9b**)] with the puckering parameters [53]. All of the six-membered spiro-rings are in chair conformations (Figs. S6b–S11b). Additionally, the five-membered spiro rings of compounds (**6b**, **9b** and **10a**) are in half-chair conformations, while the five-membered spiro rings compounds (**7b**, **9a** and **10b**) are in envelope conformations with the puckering parameters of $\varphi = 56.5(8)°$, $\varphi = 58.7(3)°$, $\varphi = 90.2(5)°$, $\varphi = 280.4(5)°$, $\varphi = 258.1(2)°$ and $\varphi = 245.0(3)°$, respectively. Atoms C13, C14 and

Table 2 Lifetime and CHISQ values of the compounds

	6a	6b	7a	7b	8b	9a	9b	10a	10b	11a	11b
τ_F (ns)	5.69	5.78	5.76	5.87	5.74	5.77	5.77	5.77	5.87	5.65	5.88
CHISQ	1.126	1.473	1.279	1.491	1.376	1.226	1.517	1.088	1.475	1.139	1.319

Dichloromethane

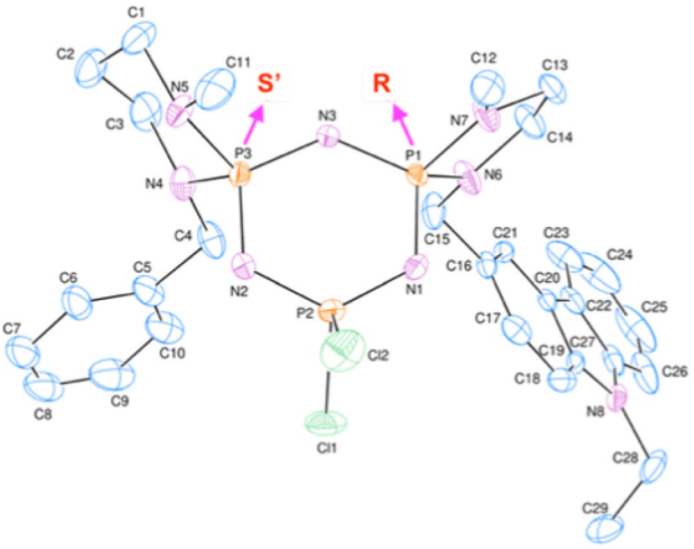

Fig. 4 ORTEP-3 [62] drawing of cis-**6b** with the atom numbering scheme. Displacement ellipsoids are drawn at the 30% probability level. Hydrogen atoms have been omitted for clarity

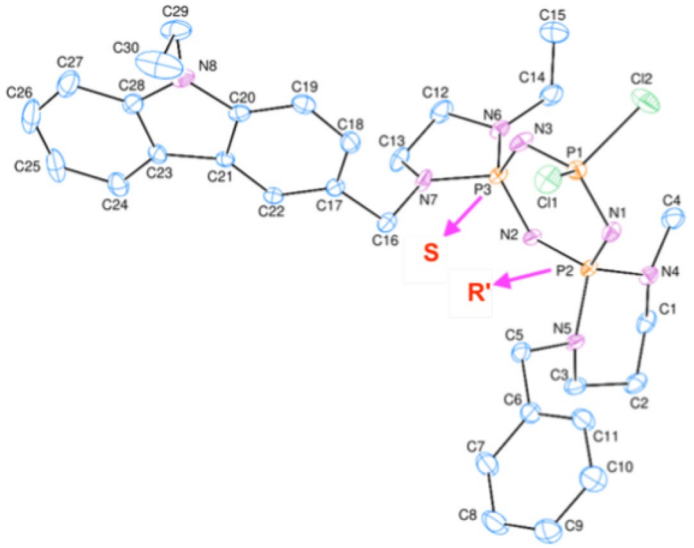

Fig. 5 ORTEP-3 [62] drawing of cis-**7b** with the atom numbering scheme. Displacement ellipsoids are drawn at the 30% probability level. Hydrogen atoms have been omitted for clarity

C2 are in flap positions and they are 0.7188(35) Å (for **7b**), −0.4976(20) Å (for **9a**) and −0.5194(20) Å (for **10b**) away from the best least-squares planes of the other four atoms of the corresponding rings in envelope conformations. On the other hand, the X-ray crystallography is used to evaluate the chiral properties of phosphazenes

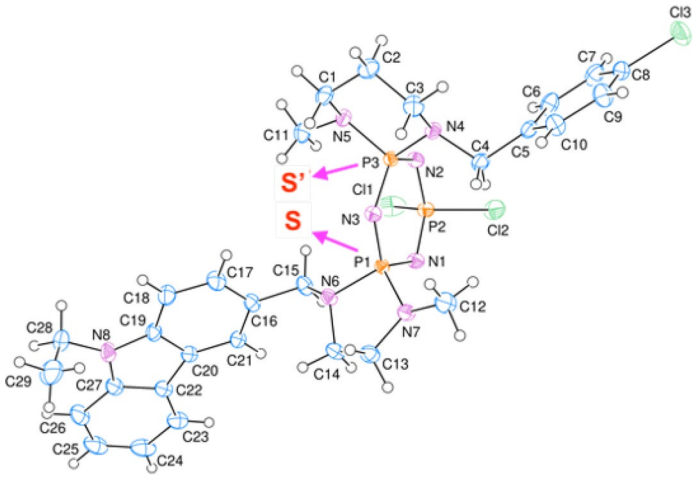

Fig. 6 ORTEP-3 [62] drawing of trans-**9a** with the atom numbering scheme. Displacement ellipsoids are drawn at the 30% probability level

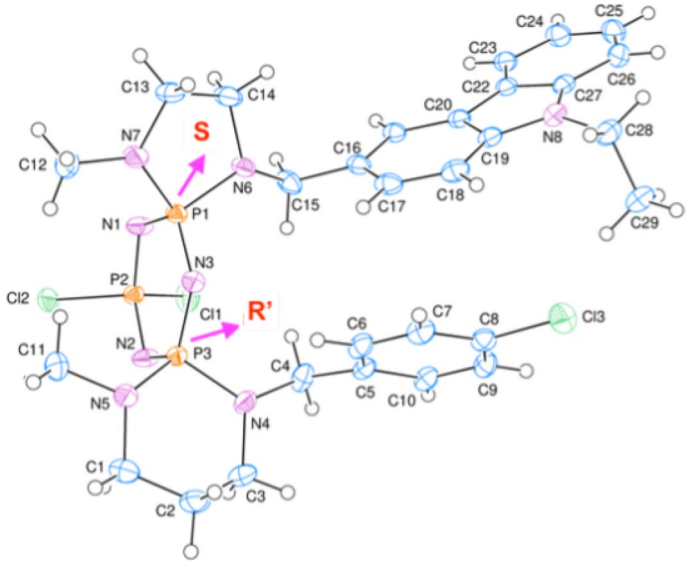

Fig. 7 ORTEP-3 [62] drawing of cis-**9b** with the atom numbering scheme. Displacement ellipsoids are drawn at the 30% probability level

containing stereogenic centers. The space groups of the compounds were determined as *P -1* (for cis-**6b**, trans-**9a**, cis-**9b** and cis-**10b**), $P\,2_12_12_1$ (for cis-**7b**) and $P\,2_1/c$ (and $P2_1/c$ (for trans-**10a**) (Table S4). The space groups *P -1* and $P\,2_1/c$ are centrosymmetric and therefore do not belong to the "Sohncke" space groups [20, 54]. Compounds with these space groups must contain both enantiomers in the unit cells

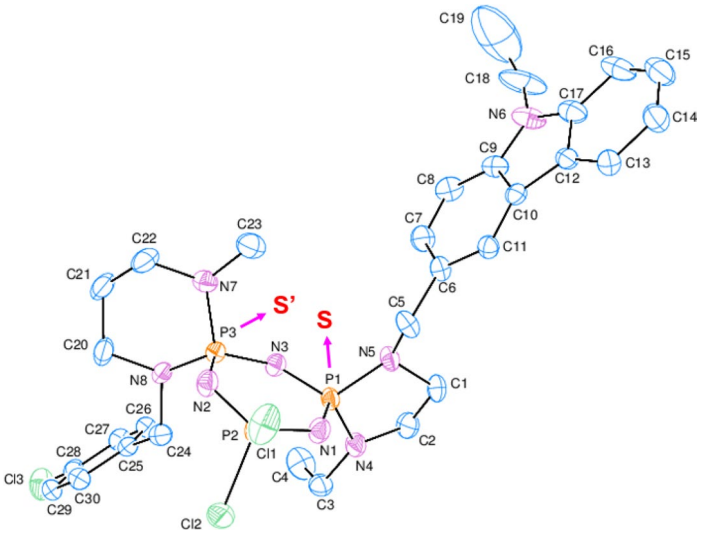

Fig. 8 ORTEP-3 [62] drawing of trans-**10a** with the atom numbering scheme. Displacement ellipsoids are drawn at the 30% probability level. Hydrogen atoms have been omitted for clarity

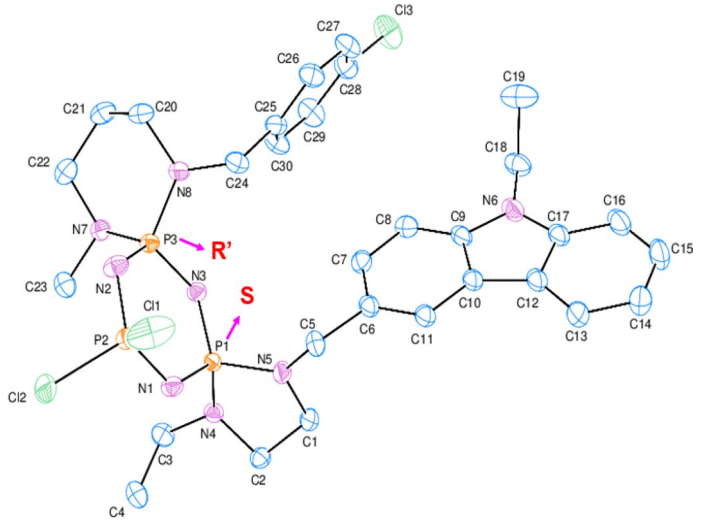

Fig. 9 ORTEP-3 [62] drawing of cis-**10b** with the atom numbering scheme. Displacement ellipsoids are drawn at the 30% probability level. Hydrogen atoms have been omitted for clarity

of their crystal lattices. Also, the absolute configurations of stereogenic phosphorus atoms can be determined by X-ray crystallography. Thus, the absolute configurations of the stereogenic phosphorus atoms of each of the enantiomers of cis-**6b**, trans-**9a**, cis-**9b**, trans-**10a** and cis-**10b**, which are racemic mixtures, were determined as RS', SR', SS', SR', SS' and SR', respectively. The absolute configurations

of the other enantiomers must be SR', RS', RR', RS', RR' and RS'. However, X-ray structure analysis revealed that cis-**7b** crystallizes as a "**pseudomeso racemate**" of chiral crystals in the orthorhombic noncentrosymmetric space group $P2_12_12_1$ ($Z=4$, $Z'=2$). Therefore, this space group belongs to the "Sohncke" groups [20, 54, 55]. The 65 "Sohncke" space group, which does not contain any mirrors, inversion points, improper rotations or glide planes, yield chiral crystals, that are not mirror image identical. While one enantiomer is usually expected in the asymmetric unit cell, among the "Sohncke" groups there are 22 consisting of 11 enantiomorphic pairs. The Flack absolute structure parameter [54, 56] of cis-**7b** is refined; expected values are X = 0.00 for the correct absolute structure and x = 1.00 for the inverted structure. The refined value is X = 0.08(5). Thus, the absolute structure (R'S) is determined reliably (Fig. 5). The absolute configuration of the other enantiomer must be (S'R). On the other hand, these enantiomers cannot transform unless the steric hindrances and spiro ring bonds of bulky groups are broken and rearranged. Therefore, they can be expected to be very stable and have quite long half-lives.

In addition, the phosphazene, N_3P_3, rings of cis-**6b** and trans-**9a** have a pseudo-mirror plane passing through the N1 and P3 atoms, but the phosphazene, N_3P_3, rings of cis-**7b**, cis-**9b**, trans-**10a** and cis-**10b** do not have a pseudo-symmetry plane (Fig. S12). The endocyclic and exocyclic bond lengths and angles of the N_3P_3 rings of the dispirophosphazenes were presented in Table S5. It was determined that the exo (γ') and endocyclic (γ) bond angles of these compounds were in the ranges of 93.26(8)°–102.67(7)° and 112.45(8)°–114.46(8)°, respectively. Compared to the bond angles of the starting compound **HCCP** [α, α', β and δ: 118.3(2)°, 101.2(1)°, 121.4(1)° and 121.4(1)°] [57], the NPN bond angles (γ and γ') significantly narrowed due to the electronic effects of the pendant arms bonded to the spiro rings. On the other hand, the endocyclic PNP bond angles (β and δ) of the dispirophosphazenes were assigned between 119.79(17)° and 128.42(9)°. However, endocyclic PNP bond angles (δ) have enlarged considerably due to the steric interactions. Besides, it was found that the endocyclic and exocyclic P–N bond lengths of the compounds varied between 1.552(3)–1.6311(15) Å and 1.6318(14)–1.6631(16) Å, respectively. It is clear that the endocyclic P–N bond lengths are significantly shorter than the exocyclic ones, as expected (Table S5). Furthermore, Table 3 summarizes the crystallographic data of some newly synthesized and analog non-symmetrical cis/trans-dispirocyclotriphosphazenes found in the literature. The table represents significantly changes in the space groups, crystal systems, N_3P_3 ring conformations, bond angles and endo/exocyclic P–N bond lengths of the compounds. These variations can be attributed to the conformation of the phosphazene and spiro rings, types of substituents, and negative hyperconjugation [58–61].

In crystal structure of **9b**, the intermolecular C—H···Cl hydrogen bonds (Table S6) link the molecules into infinite chains along the *a*-axis direction (Fig. S10c). On the other hand, in the crystal structure of **10b**, the intermolecular C—H···N and C—H···Cl hydrogen bonds (Table S6) link the molecules, enclosing $R_2^2(10)$ and $R_4^4(26)$ ring motifs, into infinite double-chains along the *a*-axis direction (Fig. S11c). The weak C—H···π interactions (Table S6) are also observed in the crystal structures of compounds (**6b**, **7b**, **9a**, **10a** and **10b**), in which they may be effective in the stabilizations of the structures.

Table 3 Crystallographic data of unsymmetrical dispirophosphazenes

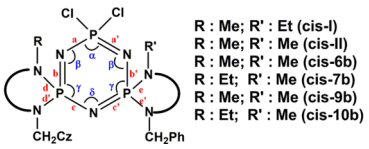

R : Me; R' : Et (cis-I)
R : Me; R' : Me (cis-II)
R : Me; R' : Me (cis-6b)
R : Et; R' : Me (cis-7b)
R : Me; R' : Me (cis-9b)
R : Et; R' : Me (cis-10b)

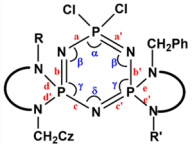

R : Me; R' : Et (trans-I)
R : Me; R' : Me (trans-9a)
R : Et; R' : Me (trans-10a)

Comp	Space group	Crystal system	N_3P_3 Ring	Q_T, φ_2 (Å, °)	Characteristic bond lenghts (°) and bond angles (Å)								
					a,a′	b,b′	c,c′	d,d′	e,e′	*α*	*β*	*γ*	*δ*
trans-**I***	C 2/c	Monoclinic	tb	0.149 (2)	1.561 (2)	1.613 (2)	1.581 (2)	1.633 (2)	1.639 (2)	121.66 (11)	120.34 (13)	113.02 (11)	128.74 (14)
				256.3 (7)	1.560 (2)	1.618 (2)	1.590 (2)	1.645 (2)	1.645 (2)		120.93 (12)	113.19 (11)	
cis-**I***	*P* bca	Orthorhombic	ft	0.127 (1)	1.5576 (15)	1.6166 (15)	1.5891 (15)	1.6557 (14)	1.6400 (15)	121.40 (8)	121.24 (9)	113.29 (8)	128.00 (9)
				65.6 (6)	1.5632 (15)	1.6171 (15)	1.5997 (15)	1.6427 (15)	1.6444 (15)		121.45 (9)	113.25 (8)	
cis-**II****	*P* -1	Triclinic	tb	0.200 (1)	1.5675 (16)	1.6241 (16)	1.5907 (15)	1.6391 (17)	1.6443 (16)	121.18 (9)	119.86 (10)	112.74 (8)	128.69 (10)
				97.8 (5)	1.5653 (16)	1.6246 (17)	1.5969 (15)	1.6434 (16)	1.6526 (17)		120.24 (10)	113.27 (8)	
cis-**6b**	*P -1*	Triclinic	fb	0.027 (2)	1.5569 (17)	1.6106 (17)	1.5829 (14)	1.6388 (16)	1.6517 (16)	121.91 (8)	120.55 (9)	112.57 (8)	128.42 (9)
				70.8 (2.6)	1.5620 (15)	1.6033 (15)	1.5940 (14)	1.6344 (16)	1.6526 (16)		122.26 (10)	114.22 (8)	
cis-**7b**	$P\,2_12_12_1$	Orthorhombic	fb	0.052 (2)	1.552 (3)	1.609 (3)	1.583 (2)	1.635 (3)	1.651 (3)	122.27 (19)	120.7 (2)	112.48 (18)	128.3 (2)
				23.0 (2.6)	1.557 (3)	1.623 (3)	1.596 (2)	1.637 (3)	1.658 (2)		121.9 (2)	114.07 (17)	
trans-**9a**	*P -1*	Triclinic	fb	0.144 (1)	1.5626 (14)	1.6222 (14)	1.5843 (13)	1.6572 (13)	1.6584 (13)	121.85 (7)	120.44 (9)	113.00 (7)	127.61 (8)
				52.7 (4)	1.5645 (13)	1.6095 (14)	1.6027 (13)	1.6485 (14)	1.6511 (13)		121.10 (8)	114.33 (7)	
cis-**9b**	*P -1*	Triclinic	sb	0.129 (1)	1.5633 (13)	1.6187 (14)	1.5877 (13)	1.6607 (13)	1.6460 (13)	121.60 (7)	120.61 (8)	113.08 (7)	128.29 (8)
				85.3 (5)	1.5635 (13)	1.6263 (13)	1.5924 (13)	1.6318 (14)	1.6557 (14)		121.11 (8)	113.75 (7)	
trans-**10a**	$P\,2_1/c$	Monoclinic	fb	0.175 (2)	1.558 (3)	1.614 (3)	1.582 (3)	1.646 (3)	1.646 (3)	120.85 (15)	119.79 (17)	112.95 (14)	127.65 (17)
				− 49.8 (8)	1.563 (3)	1.627 (3)	1.595 (3)	1.652 (3)	1.66383)		121.59 (17)	114.27 (14)	

Table 3 (continued)

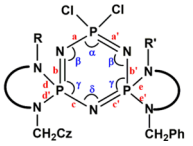

R : Me; R' : Et (cis-I)
R : Me; R' : Me (cis-II)
R : Me; R' : Me (cis-6b)
R : Et; R' : Me (cis-7b)
R : Me; R' : Me (cis-9b)
R : Et; R' : Me (cis-10b)

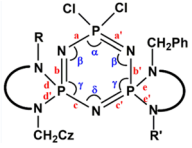

R : Me; R' : Et (trans-I)
R : Me; R' : Me (trans-9a)
R : Et; R' : Me (trans-10a)

Comp	Space group	Crystal system	N_3P_3 Ring	Q_T, φ_2 (Å, °)	Characteristic bond lenghts (°) and bond angles (Å)								
					a,a′	b,b′	c,c′	d,d′	e,e′	α	β	γ	δ
cis-**10b**	*P -1*	Triclinic	fb	0.107 (1)	1.5614 (16)	1.6200 (15)	1.5885 (15)	1.6504 (16)	1.6631 (16)	121.28 (8)	120.43 (10)	112.45 (8)	127.78 (9)
				45.3 (7)	1.5591 (16)	1.631 (15)	1.5952 (15)	1.6429 (16)	1.6437 (15)		122.73 (9)	114.46 (8)	

tb, twisted-boat; ft, flattened-boat; sc, screw-boat

*Taken from literature [38]. **Taken from literature [14]

Antimicrobial activity

To determine the anti-microbiological activities of the dispirophosphazenes (**6a**–**11a** and **6b**–**11b**) at a concentration of 2500 µM, ten pathogenic bacteria [*Staphylococcus aureus* (ATCC 25923), *Bacillus cereus* (NRRL B-3711), *Bacillus subtilis* (ATCC 6633), *Escherichia coli* (ATCC 35218, 25922), *Enterococcus faecalis* (ATCC 29212), *Pseudomonas aeruginosa* (ATCC 27853), *Klepsiella pneumaniae* (ATCC 13883), *Salmonella typhimurium* (ATCC 14028), *Enterococcus hirae* (ATCC 9790) and *Proteus vulgaris* (RSKK 96029)] and three yeast strains [*Candida albicans* (ATCC 10231), *Candida krusei* (ATCC 6258) and *Candida tropicalis* (Y-12968)] were used in the agar well diffusion method. Ampicillin (10 µg), Chloramphenicol (30 µg) and Ketoconazole (50 µg), the commercially available antibiotics, were utilized as controls. According to the results obtained, compounds were effective, except cis-**7b**. Compound **7b** had a weak activity against *S. aureus*. Besides, dispirophosphazenes did not show any activity against *E. coli* strains, *P. aeruginosa* and *K. pneumaniae*. Compounds did not have efficient growth inhibition on yeast species *C. albicans*, *C. Krusei* and *C. tropicalis*, except **8a** and **8b**. Compounds **8a** (15 ± 1) and **8b** (16 ± 1) have better growth inhibition against *C. albicans* than that of the control antibiotic (11 ± 1) (Table S7).

The minimum inhibitory concentrations (MICs), defined as the lowest concentration that prevents to growth of microoorganisms, were determined for dispirophosphazenes (Table S8). The concentrations of **6a**–**11a** and **6b**–**11b** were ranged from 156.3 to 2500 µM.

On the other hand, the Minimum Bactericidal and Fungicidal Concentrations (MBC and MFC) indicate the minimum concentrations of antimicrobial agents that decrease the viability of initial microorganism numbers of 99.9%. According to MIC, MBC and MFC values (Table S9), compounds were not effective against *B. subtilis*, *B. cereus*, *S. aureus*, *E. faecalis*, *S.typhimurium* and *E. hirae*. According to the determined MBC values, all compounds were more efficient than positive controls against *K. pneumaniae* and all compounds have better activity than positive controls against *E. coli 35218* except for cis-**6b** and trans-**9a**. However, compounds were found to have even better activities on *P. aeruginosa* than the positive controls. The lowest MBC value was determined as 78.1 µM against *B. cereus* for trans-**8a**.

The antimicrobial activities of symmetrical dispirophosphazenes containing 4-substituted(X)-benzyl pendant arms (X:H, Cl and OCH_3) were determined against eleven bacteria and three yeasts [39, 58, 63, 64]. In addition, unsymmetrical dispirophosphazenes decorated with carbazolyl and benzyl/4-chloro-benzyl pendants have also been reported to have antimicrobial activity [14, 38]. Table 4 lists symmetrical and unsymmetrical dispirocyclotriphosphazenes containing pendant arms with antimicrobial activity equal to or greater than standard antibiotics (amphicilin and chloramphenicol). Symmetrical dispirophosphazenes are effective against two G(+) and five G(−) bacteria, while unsymmetrical derivatives are effective against four G(−) bacteria. It should be stated that *B. cereus*, *E. hirae* and *S. typhimurium* were susceptible to 4-Cl(N/N) benzyldispirocyclotriphosphazenes but ineffective to unsymmetrical dispiro ones. Another important result is that the unsymmetrical derivatives are specifically active against *P. aeruginosa*. Moreover, all symmetrical

Table 4 Symmetrical and unsymmetrical dispirocyclotriphosphazenes containing pendant-arms with antimicrobial activity equal to or greater than standard antibiotics*. (x: active)

Test organisms	Symmetrical dispirophosphazenes				Unsymmetrical dispirophosphazenes with carbazolyl and benzyl/4-chloro-benzyl pendant arms (N/N)[e]
	Benzyl (N/O)[a]	4-Chloro-benzyl (N/N)[b]	(N/O)[c]	4-Methoxy-benzyl (N/N)[d]	
B. cereus G(+)		x	x		
E. coli 35218 G(−)		x	x	x	x
E. hirae G(+)		x			
K. pneumaniae G(−)	x		x		x
P. aeruginosa G(−)					x
P. vulgaris G(−)	x				x
S. typhimurium G(−)		x			
C. albicans		x	x	x	

Standard antibiotics: Amphicilin and Chloramphenicol for bacteria and Ketoconazole for yeast strains
[a][63]; [b][39]; [c][58]; [d][64]; [e][14, 38] and this study

(except benzyl groups) and unsymmetrical dispirophosphazenes are active against *E. coli 35218* according to Table 4. Likewise, it should be emphasized that *C. albicans* is susceptible to 4-Cl(N/N), 4-Cl(N/O) and 4-OCH_3(N/N) benzyldispirophosphazenes. Therefore, these derivatives can be proposed as anti-candidal compounds.

Interactions of PBR322 DNA with the phosphazene derivatives

Untreated plasmid DNA has two bands which are (Form I and Form II). Form III band occurs under the influence of DNA damage. As a result of damage of dispirophosphazenes on plasmid DNA, double-strand cleavage can occur, and a linear DNA band can emerge on the agarose gel. Dispirophosphazenes (**6a**–**11a** and **6b**–**11b**) with DNA interaction were evaluated using agarose gel electrophoresis method. The concentrations of compounds were ranging from 2500 to 156.3 µM. The compounds (trans-**8a**, cis-**8b** and trans-**9a**) did not possess any DNA band at the highest concentration of 2500 µM (Fig. S13). The compounds trans-**6a**, trans-**7a**, cis-**9b**, trans-**10a** and cis-**11b** induced decreases in concentrations of form I and induced increases in concentrations of form II by cleavage of one strand DNA. The linear band was also observed in compounds (trans-**7a**, trans-**9a** and trans-**10a**) showing double-strand cleavage.

Restriction endonuclease reaction with *BamH*I and *Hind*III enzyme

*BamH*I and *Hind*III are restriction endonuclease enzymes that hydrolyze the phosphodiester bonds in DNA. The recognition sites are 5′-G/GATCC-3′ and 5′-A/AGCTT-3′ sequences, and cut from 5′-guanine for *BamH*I and 5′ adenine for *Hind*III enzyme. pBR322 plasmid DNA has a single restriction site that makes it into

a supercoiled form I and circular form II to linear form III DNA for two enzymes. The linear form III was generated when plasmid DNA was restricted with restriction endonucleases without compounds. In this study, the interaction evaluations between the compounds (trans **6a–11a** and cis **6b–11b**) and guanine-guanine (G/G) and/or adenine-adenine (A/A) regions of DNA were performed through restriction endonuclease analyses of the compound-plasmid DNA adducts by *Hind*III and *BamH*I enzymes. *BamH*I and *Hind*III enzymes partly restrict plasmid DNA interacting with compounds, indicating all the compounds binding DNA (Fig. 10).

Conclusion

This study was aimed to synthesize and determine the spectral characterizations, stereogenic and photophysical properties, and biological activities of the unsymmetrical inorganic–organic hybrid cis/trans cyclotriphosphazenes containing different pendant arms. The reactions of monospirocyclotriphosphazenes (**1** and **2**) with the carbazolyldiamines (**3–5**) produce unsymmetrical cis (**6a–11a**) and trans (**6b–11b**) dispirocyclotriphosphazenes containing carbazolyl and benzyl/4-chlorobenzyl pendant arms. Their spectral properties were revealed using elemental analysis, FTIR, APIES-MS and NMR spectroscopic methods. The stereogenisms of dispirophosphazenes were explored by CD and CSA-added ^{31}P NMR spectra. The absolute configurations of cis-**6b**, cis-**7b**, trans-**9a**, cis-**9b**, trans-**10a** and cis-**10b** were found as RS', SR', SS', SR', SS' and SR' according to the X-ray results, respectively. These findings indicate that the compounds are in racemates. It is determined that these results are compatible with each other. The space groups *P -1* and *P* $2_1/c$ belonging to cis-**6b**, trans-**9a**, cis-**9b,** cis-**10b** and trans-**10a** are not in the Sohncke space, groups, while the space group *P* $2_12_12_1$ for cis-**7b** is in the Sohncke groups. Moreover, The Flack parameter of cis-**7b** is found to be 0.08(5) indicating that the absolute configuration found from the X-ray data is accurate. On the other hand, the photophysical

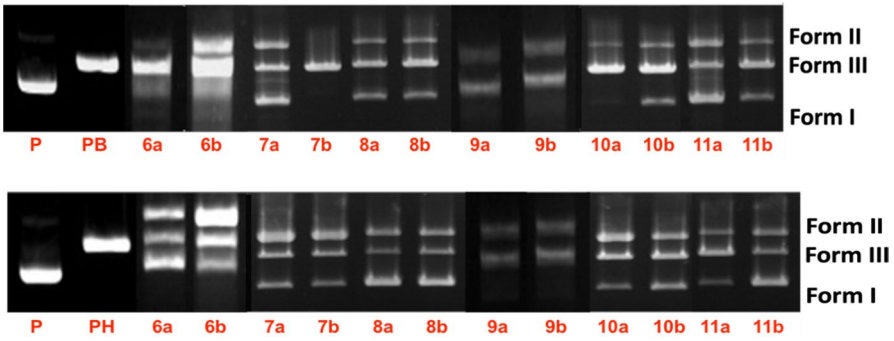

Fig. 10 Electrophoretograms applying to the incubated mixtures of pBR322 plasmid DNA and compounds (**6a–11a** and **6b–11b**) followed by digestion with *BamH*I and *Hind*III. Lane P1 applied to the untreated pBR322 plasmid DNA and undigested with enzyme, lane P/B and P/H applied to untreated but digested with *BamH*I and *Hind*III, respectively

properties of the compounds were clarified using UV/vis and both steady-state and time-resolved fluorescence measurements. The data show that the compounds have the fluorescence half-life time (τ_F) ranging from 5.6 to 5.9 ns. Additionally, the τ_F (ns) and CHISQ values of the trans-isomers (**6a–11a**) were found to be significantly smaller than the values of the cis-isomers (**6b–11b**). Moreover, the MIC, MBC and MFC values of all dispirophosphazenes were also determined. The antimicrobial activities of some cis/trans-isomers appear to be quite different and greater against some bacterial and yeast species. For example, trans-**8a** is very active against B. cereus (MBC = 78.1 μM). While, cis-**6b**, trans-**9a** and cis-**9b** are significantly active against the pathogenic yeast C. albicans (MFC = 156.3 μM). The compound-DNA interactions were investigated using agarose gel electrophoresis method. All dispirophosphazenes were found to bind to A/A and G/G nucleotides DNA with respect to the restriction endonuclease experiments with *BamH*I and *Hind*III enzymes.

Supplementary Information The online version contains supplementary material available at https://doi.org/10.1007/s11164-024-05285-7.

Acknowledgements Z. K. thanks the Turkish Academy of Sciences (TÜBA) for partial support of this work.

Author contributions RC: formal analysis, ınvestigation, writing–original draft, visualization. NA: conceptualization, methodology, formal analysis, resources, writing-original draft, writing–review and editing, project administration. ZK: conceptualization, methodology, writing–original draft, writing–review and editing, project administration. BTA: ınvestigation, writing–original draft. BNS: ınvestigation, writing–original draft. LA: ınvestigation, writing–original draft, writing–review and editing. TH: ınvestigation, formal analysis, writing–original draft, writing–review and editing.

Funding Open access funding provided by the Scientific and Technological Research Council of Türkiye (TÜBİTAK). The authors acknowledge the Scientific and Technical Research Council of Turkey Grant No. 122Z180. T. H. is grateful to Hacettepe University Scientific Research Project Unit (Grant No. 013 D04 602 004).

Availability of data and materials Not applicable.

Declarations

Competing interests The authors declare that they have no known competing financial interests or personal relationships that could have appeared to influence the work reported in this paper.

Ethical approval Not applicable.

References

1. Y. Tümer, N. Asmafiliz, G. Arslan, Z. Kılıç, T. Hökelek, J. Mol. Struct. **1181**, 235 (2019)
2. Y. Tümer, N. Asmafiliz, Z. Kılıç, B. Aydın, L. Açık, T. Hökelek, J. Mol. Struct. **1173**, 885 (2018)
3. C.M. Balcı, D. Palabıyık, S. Beşli, Inorg. Chim. Acta **521**, 120317 (2021)
4. N. Asmafiliz, Z. Kılıç, M. Civan, O. Avcı, L.Y. Gönder, L. Açık, B. Aydın, M. Türk, T. Hökelek, New J. Chem. **40**, 9609 (2016)
5. S. Türe, C. Darcan, O. Türkyılmaz, Ö. Kaygusuz, Phosphorus Sulfur Silicon Relat. Elem. **195**(6), 507 (2020)
6. İ Berberoğlu, R. Cemaloğlu, N. Asmafiliz, Z. Kılıç, C.T. Zeyrek, L. Açık, D. Koyunoğlu, M. Türk, T. Hökelek, Res. Chem. Intermed. **48**, 3189 (2022)
7. R. Cemaloğlu, İ Berberoğlu, N. Asmafiliz, Z. Kılıç, T. Hökelek, J. Mol. Struct. **1269**, 133866 (2022)
8. N.S. Başterzi, S. Bilge Koçak, A. Okumuş, Z. Kılıç, T. Hökelek, Ö. Çelik, M. Türk, L.Y. Koç, L. Açık, B. Aydın, New J. Chem. **39**, 8825 (2015)
9. N. Asmafiliz, Z. Kılıç, A. Öztürk, Y. Süzen, T. Hökelek, L. Açık, Z.B. Çelik, L.Y. Koç, M.L. Yola, Z. Üstündağ, Phosphorus Sulfur Relat. Elem. **188**, 1723 (2013)
10. E.E. İlter, N. Çaylak, M. Işıklan, N. Asmafiliz, Z. Kılıç, T. Hökelek, J. Mol. Struct. **697**, 119 (2004)
11. A. Okumuş, S. Bilge, Z. Kılıç, A. Öztürk, T. Hökelek, F. Yılmaz, Spectrochim. Acta A Mol. Biomol. Spectros. **76**, 401 (2010)
12. N. Uzunalioğlu, N. Asmafiliz, Z. Kılıç, T. Hökelek, Inorg. Chim. Acta **539**, 121035 (2022)
13. N. Asmafiliz, Heteroat. Chem. **25**, 83 (2014)
14. R. Cemaloğlu, N. Asmafiliz, B. Çoşut, Z. Kılıç, B.N. Sabah, L. Açık, H. Mergen, T. Hökelek, Res. Chem. Intermed. **49**, 2071 (2023)
15. G. Elmas, A. Binici, M. Yakut, A. Okumuş, Z. Kılıç, B. Çoşut, T. Hökelek, N.A. Çerçi, L. Açık, New J. Chem. **46**, 16096 (2022)
16. G. Elmas, Phosphorus Sulfur Relat. Elem. **194**, 13 (2018)
17. G. Casella, S. Carlotto, F. Lanero, M. Mozzon, P. Sgarbossa, R. Bertani, Molecules **27**(23), 8117 (2022)
18. S. Orlandini, G. Hancu, Z.I. Szabo, A. Modroiu, L.A. Papp, R. Gotti, S. Furlanetto, Molecules **27**(20), 7058 (2022)
19. N. Bodor, P. Buchwald, Med. Res. Rev. **20**(1), 58 (2000)
20. E. Pidcock, Chem. Commun. **27**, 3457 (2005)
21. K.A. Solomon, MJP Publisher (2019)
22. M.M. Coelho, C. Fernandes, F. Remiao, M.A. Tiritan, Molecules **26**(11), 3113 (2021)
23. V.V.S.P.K. Rayala, J.S. Kandula, R. Pullapanthula, Chirality **34**, 1298 (2022)
24. J.S. Kandula, V.V.S.P.K. Rayala, R. Pullapanthula, Sep. Sci. Plus **6**, 2200131 (2023)
25. B. Dhakal, Y. Tomita, P. Drew, T. Price, G. Maddern, E. Smith, K. Fenix, Molecules **28**, 3624 (2023)
26. T. Eriksson, S. Björkman, P. Höglund, Eur. J. Clin. Pharmacol. **57**, 365 (2001)
27. T. Paravar, D.J. Lee, Int. Rev. Immunol. **27**, 111 (2008)
28. J. Jan-Roblero, J.A. Cruz-Maya, Molecules **28**, 2097 (2023)
29. S. Al-Sulaimi, R. Kushwah, M. Abdullah Alsibani, A. El Jery, M. Aldrdery, G.A. Ashraf, Molecules **28**, 6175 (2023)
30. M.S. Sinicropi, D. Iacopetta, C. Rosano, R. Randino, A. Caruso, C. Saturnino, N. Muia, J. Ceramella, F. Puoci, M. Rodriquez, P. Longo, M.R. Plutino, J. Enzyme Inhib. Med. Chem. **33**(1), 434 (2018)
31. C. Saturnino, A. Caruso, D. Iacopetta, C. Rosano, J. Ceramella, N. Muià, A. Mariconda, M.G. Bonomo, M. Ponassi, G. Rosace, M.S. Sinicropi, P. Longo, ChemMedChem **13**(24), 2635 (2018)
32. A. Panno, M.S. Sinicropi, A. Caruso, H. El-Kashef, J.C. Lancelot, G. Aubert, A. Lesnard, T. Cresteil, S. Rault, J. Heterocycl. Chem. **51**(S1), E294 (2014)
33. G. Hao, J. Sun, C. Wei, Bioorg. Med. Chem. **26**(1), 285 (2018)
34. S.A. Patil, S.A. Patil, E.A. Ble-González, S.R. Isbel, S.M. Hampton, A. Bugarin, Molecules **27**, 6575 (2022)
35. D. Palabıyık, C. Mutlu Balcı, S.O. Tümay, I.F. Şengül, S. Beşli, Inorg. Chim. Acta **539**, 121022 (2022)
36. R. Kumar Konidena, J. Thomas, J. Wook Park, ChemPhotoChem **6**, e202200059 (2022)
37. H. Akbaş, J. Mol. Struct. **1200**, 127079 (2020)

38. R. Cemaloglu, N. Asmafiliz, Z. Kılıç, B. Çoşut, B.N. Sabah, L. Açık, N.A. Çerçi, T. Hökelek, New J. Chem. **47**, 1900 (2023)
39. N. Asmafiliz, İ Berberoğlu, M. Özgür, Z. Kılıç, H. Kayalak, L. Açık, M. Türk, T. Hökelek, Inorg. Chim. Acta **495**, 118949 (2019)
40. B.M. Trost, M.T. Sorum, Org. Process Res. Dev. **7**, 432 (2003)
41. B.M. Trost, Acc. Chem. Res. **29**, 8 (1996)
42. A. Uslu, S. Yeşilot, Coord. Chem. Rev. **291**, 28 (2015)
43. Ş Şahin Ün, A. Uslu, S. Yeşilot, İ Ün, B. Çoşut, F. Yuksel, A. Kılıç, Polyhedron **30**(9), 1587 (2011)
44. S. Beşli, S.J. Coles, L.S. Coles, D.B. Davies, A. Kılıç, Polyhedron **43**(1), 176 (2012)
45. N.S. Kumar, K.K. Swamy, Polyhedron **23**(6), 979 (2004)
46. M. Willson, L. Lafaille, G. Commenges, J.F. Labarre, Phosphorus Sulfur Silicon Relat. Elem. **25**(3), 273 (1985)
47. R. Cemaloğlu, İ Berberoğlu, M. Yakut, A. Binici, N. Asmafiliz, Z. Kılıç, R. Güzel, G. Erdal, H. Şimşek, T. Hökelek, New J. Chem. **47**, 19788 (2023)
48. A. Ault, J. Chem. Educ. **85**(3), 441 (2008)
49. H. Ardıç Alidağı, F. Hacıvelioğlu, S.O. Tümay, B. Çoşut, S. Yeşilot, Inorg. Chim. Acta **457**, 95 (2017)
50. T. Nishimoto, T. Yasuda, S.Y. Lee, R. Kondo, C. Adachi, Mater. Horiz. **1**, 264 (2014)
51. M.S. Soh, S.A.G. Santamaria, E.L. Williams, M.P. Morales, H.J. Bolink, A. Sellinger, J. Polym. Sci. B Polym. Phys. **49**, 531 (2011)
52. S.I. Kato, H. Noguchi, A. Kobayashi, T. Yoshihara, S. Tobita, Y. Nakamura, J. Org. Chem. **77**(20), 9120 (2012)
53. D. Cremer, J.A. Pople, J. Am. Chem. Soc. **97**, 1354 (1975)
54. H.D. Flack, Helv. Chim. Acta **86**, 905 (2003)
55. T. Rekis, J. Appl. Cryst. **56**, 322 (2023)
56. S. Parsons, H.D. Flack, T. Wagner, Acta Cryst. **B69**, 249 (2013)
57. G.J. Bullen, J. Chem. Soc. A Inorg. Phys. Theor. 1450 (1971)
58. Ö. İşcan, R. Cemaloğlu, N. Asmafiliz, C.T. Zeyrek, Z. Kılıç, L. Açık, B. Aydın, M. Türk, T. Hökelek, Mol. Divers. **26**(2), 1077 (2022)
59. A.B. Chaplin, J.A. Harrison, P.J. Dyson, Inorg. Chem. **44**(23), 8407 (2005)
60. R.P. Orenha, R. Vessecchi, S.E. Galembeck, Struct. Chem. **29**(3), 847 (2018)
61. N. Güven Kuzey, M. Özgür, R. Cemaloğlu, N. Asmafiliz, Z. Kılıç, L. Açık, B. Aydın, T. Hökelek, J. Mol. Struct. **1220**, 128658 (2020)
62. L.J. Farrugia, J. Appl. Crystallogr. **45**(4), 849 (2012)
63. Ö. İşcan, R. Cemaloğlu, N. Asmafliz, Z. Kılıç, L. Açık, P. Özbeden, T. Hökelek, Turk. J. Chem. **44**, 15 (2020)
64. N. Kuzey Güven, M. Özgür, R. Cemaloğlu, N. Asmafliz, Z. Kılıç, L. Açık, B. Aydın, T. Hökelek, Res. Chem. Intermed. **47**, 3933 (2021)

Authors and Affiliations

Reşit Cemaloğlu[1,2] · Nuran Asmafiliz[1] · Zeynel Kılıç[1] · Burcu Topaloğlu Aksoy[3] · Büşra Nur Sabah[4] · Leyla Açık[4] · Tuncer Hökelek[5]

✉ Nuran Asmafiliz
gurun@science.ankara.edu.tr

[1] Department of Chemistry, Ankara University, 06100 Ankara, Turkey

[2] Department of Chemistry, Graduate School of Natural and Applied Sciences, Ankara University, Ankara, Turkey

[3] Department of Chemistry, Gebze Technical University, 41400 Gebze-Kocaeli, Turkey

[4] Department of Biology, Gazi University, 06500 Ankara, Turkey

[5] Department of Physics, Hacettepe University, 06800 Beytepe, Ankara, Turkey